



Estimating UK
greenhouse gas
emissions

A. L. Ganesan et al.

This discussion paper is/has been under review for the journal Atmospheric Chemistry and Physics (ACP). Please refer to the corresponding final paper in ACP if available.

Quantifying methane and nitrous oxide emissions from the UK using a dense monitoring network

A. L. Ganesan¹, A. J. Manning², A. Grant¹, D. Young¹, D. E. Oram³,
W. T. Sturges³, J. B. Moncrieff⁴, and S. O'Doherty¹

¹School of Chemistry, University of Bristol, Bristol, UK

²Hadley Centre, Met Office, Exeter, UK

³School of Environmental Sciences, University of East Anglia, Norwich Research Park, Norwich, UK

⁴School of Geosciences, University of Edinburgh, Edinburgh, UK

Received: 28 October 2014 – Accepted: 15 December 2014 – Published: 9 January 2015

Correspondence to: A. L. Ganesan (anita.ganesan@bristol.ac.uk)

Published by Copernicus Publications on behalf of the European Geosciences Union.

Title Page

Abstract

Introduction

Conclusions

References

Tables

Figures



Back

Close

Full Screen / Esc

Printer-friendly Version

Interactive Discussion



Abstract

The UK is one of several countries around the world that has enacted legislation to reduce its greenhouse gas emissions. Monitoring of emissions has been done through a detailed sectoral level bottom-up inventory (UK National Atmospheric Emissions Inventory, NAEI) from which national totals are submitted yearly to the United Framework Convention on Climate Change. In parallel, the UK government has funded four atmospheric monitoring stations to infer emissions through top-down methods that assimilate atmospheric observations. In this study, we present top-down emissions of methane (CH_4) and nitrous oxide (N_2O) for the UK and Ireland over the period August 2012 to August 2014. We used a hierarchical Bayesian inverse framework to infer fluxes as well as a set of covariance parameters that describe uncertainties in the system. We inferred average UK emissions of 2.08 (1.72 – 2.47) Tg yr^{-1} CH_4 and 0.105 (0.087 – 0.127) Tg yr^{-1} N_2O and found our derived estimates to be generally lower than the inventory. We used sectoral distributions from the NAEI to determine whether these discrepancies can be attributed to specific source sectors. Because of the distinct distributions of the two dominant CH_4 emissions sectors in the UK, agriculture and waste, we found that the inventory may be overestimated in agricultural CH_4 emissions. We also found that N_2O fertilizer emissions from the NAEI may be overestimated and we derived a significant seasonal cycle in emissions. This seasonality is likely due to seasonality in fertilizer application and in environmental drivers such as temperature and rainfall, which are not reflected in the annual resolution inventory. Through the hierarchical Bayesian inverse framework, we quantified uncertainty covariance parameters and emphasized their importance for high-resolution emissions estimation. We inferred average model errors of approximately 20 and 0.4 ppb and correlation timescales of 1.0 (0.72 – 1.43) and 2.6 (1.9 – 3.9) days for CH_4 and N_2O , respectively. These errors are a combination of transport model errors as well as errors due to unresolved emissions processes in the inventory. We found the largest CH_4 errors at the Tacolneston station

ACPD

15, 857–886, 2015

Estimating UK greenhouse gas emissions

A. L. Ganesan et al.

Title Page

Abstract

Introduction

Conclusions

References

Tables

Figures



Back

Close

Full Screen / Esc

Printer-friendly Version

Interactive Discussion



in eastern England, which is possibly to do with sporadic emissions from landfills and offshore gas in the North Sea.

1 Introduction

Methane (CH₄) and nitrous oxide (N₂O) are the second and third most important greenhouse gases after carbon dioxide (CO₂) and have global warming potentials over a 100 year time horizon of 34 and 298, respectively (Myhre et al., 2013). Because of their importance to climate, there is considerable interest in quantifying emissions at the national level for the purposes of policy reduction measures.

In 2008, the UK brought into legislation the Climate Change Act 2008 (<http://www.legislation.gov.uk/ukpga/2008/27/contents>) with the legally binding target to reduce the country's CO₂ equivalent emissions to 80 % of 1990 levels by 2050. As part of the efforts over the past several decades to quantify emissions, the UK government produces the National Atmospheric Emissions Inventory (NAEI, <http://naei.defra.gov.uk>), which currently includes a yearly gridded 1 km x 1 km sectoral inventory of anthropogenic emissions of the major greenhouse gases (Fig. 1). National total emissions from this inventory are submitted yearly to the United Framework Convention on Climate Change (UNFCCC, www.unfccc.int), which requires developed countries to annually report their emissions of CO₂, CH₄, N₂O, sulfur hexafluoride (SF₆), hydrofluorocarbons (HFCs) and perfluorocarbons (PFCs). In 2012, the UK reported 2.42 Tgyr⁻¹ of CH₄ with an uncertainty of 20 % and 0.116 Tgyr⁻¹ of N₂O with an uncertainty of 69 % to the UNFCCC. Of the basket of gases in the inventory, N₂O is the most uncertain.

Globally, emissions of these gases to the atmosphere come from both biogenic and anthropogenic sources. In the UK however, anthropogenic sources dominate over natural sources (Table 1 and references therein). The principal sources of CH₄ in the UK in 2012, as reported from NAEI inventories, were from agriculture (44 %), waste (40 %) and energy (15 %). For N₂O, reported emissions were largely from agricultural soils (75 %), followed by fuel combustion (11 %) and animal waste management (8 %).

Estimating UK greenhouse gas emissions

A. L. Ganesan et al.

Title Page

Abstract

Introduction

Conclusions

References

Tables

Figures



Back

Close

Full Screen / Esc

Printer-friendly Version

Interactive Discussion



Estimating UK greenhouse gas emissions

A. L. Ganesan et al.

Title Page

Abstract

Introduction

Conclusions

References

Tables

Figures



Back

Close

Full Screen / Esc

Printer-friendly Version

Interactive Discussion



Alongside efforts to maintain a detailed bottom-up inventory, which compiles information using emissions factors and source information, the UK implemented four monitoring stations around the UK and Ireland to infer emissions through top-down methods using atmospheric observations. Quantification of emissions at the national level requires dense measurement networks to provide enough coverage and information to constrain fluxes at high resolution. The four greenhouse gas stations of the UK DECC (Deriving Emissions linked to Climate Change) network were situated to constrain emissions of potent greenhouse gases from the UK. These four stations are located at Mace Head (MHD, 53.33° N, 9.90° W, 25 m.a.s.l.) on the western coast of Ireland, and telecommunication towers at Ridge Hill (RGL, 52.00° N, 2.54° W, 204 m.a.s.l.) in western England, Tacolneston (TAC, 52.52° N, 1.14° E, 56 m.a.s.l.) in eastern England and Angus (TTA, 56.56° N, 2.99° W, 400 m.a.s.l.) in eastern Scotland. While operations at Mace Head have been supported by the UK government for several decades, the latter three sites were funded by the UK's Department of Energy and Climate Change beginning in 2011. With the exception of Angus, which currently only measures CO₂ and CH₄, the remaining sites are additionally equipped to monitor N₂O and SF₆.

Emissions of CH₄ and N₂O have previously been estimated both globally and regionally for the UK and Northwest Europe using inverse methods (Manning et al., 2011; Corazza et al., 2011; Bergamaschi et al., 2014). While global emissions have been estimated to be around 554 ± 56 and 15.8 ± 1.0 Tg yr⁻¹ (Prather et al., 2012), respectively, regional and national-scale emissions are significantly more uncertain. Manning et al. (2011) used a regional approach to infer emissions for the UK using measurements from Mace Head, Ireland and found the UK's contribution in 2007 to be 1.88 (0.8–3.3) Tg yr⁻¹ CH₄ and 0.070 (0.055–0.090) Tg yr⁻¹ N₂O. Bergamaschi et al. (2014), using a variety of global and regional approaches, derived 2006–2007 emissions for the UK and Ireland that ranged between 2.5–5 Tg yr⁻¹ for CH₄ and 0.07–0.17 Tg yr⁻¹ for N₂O, depending on the inversion method and chemical transport model. The large range in derived emissions, which were almost always larger than the individual uncer-

tainties of each model/inversion, highlights the need for robust uncertainty quantification and investigation into systematic model errors.

The objectives of this study were to: (1) quantify UK emissions of CH₄ and N₂O using the UK's national monitoring network for the period of August 2012 to August 2014; (2) use spatial patterns in derived emissions to understand sources of discrepancy between the top-down and bottom-up inventories at the sectoral and regional levels; (3) quantify critical uncertainty parameters, including spatially and temporally varying variances and correlations using a hierarchical Bayesian inverse method (Ganesan et al., 2014); (4) use the derived parameters to inform development of national-scale monitoring networks.

2 Measurements

Observations of atmospheric CH₄ and N₂O mole fraction have been collected since 1987 and 1978, respectively, at Mace Head, Ireland, which is one of the core long-term observatories of the Advanced Global Atmospheric Gases Experiment (AGAGE). Ambient air measurements were made on a gas chromatograph (GC, Agilent 5890) equipped with a flame ionization detector (FID, Carle) for CH₄ and electron capture detector (ECD, Agilent) for N₂O every 40 min. Standards were filled wet in electropolished stainless steel cylinders and were calibrated on the Tohoku University and SIO-98 calibration scales, respectively. A detailed description of the methodology can be found in Prinn et al. (2000).

Measurement at the telecommunications towers at Ridge Hill, Tacolneston and Angus have been made since March 2012, July 2012 and March 2011, respectively, with CH₄ measurement occurring at all three sites and N₂O measurement occurring only at Ridge Hill and Tacolneston (<http://www.metoffice.gov.uk/atmospheric-trends/>). Methane analysis was conducted using a Picarro Cavity Ring Down spectrometer (CRDS). Ridge Hill and Tacolneston were equipped with the G2301 CRDS instrument continuously over the measurement period and employed sample drying using a Nafion

Estimating UK greenhouse gas emissions

A. L. Ganesan et al.

Title Page

Abstract

Introduction

Conclusions

References

Tables

Figures



Back

Close

Full Screen / Esc

Printer-friendly Version

Interactive Discussion



Estimating UK greenhouse gas emissions

A. L. Ganesan et al.

Title Page

Abstract

Introduction

Conclusions

References

Tables

Figures



Back

Close

Full Screen / Esc

Printer-friendly Version

Interactive Discussion



membrane driven by a dry countercurrent gas. Angus measurements were made on the G1301 series until May 2013, after which, a G2301 model was installed. No sample drying was employed at this site. All measurements at these three sites were calibrated using dry standards filled in aluminum cylinders. Methane observations were calibrated on the NOAA-2004 calibration scale and were converted to the Tohoku University scale for consistency with Mace Head observations using a calibration factor of 1.0003. Sampling heights on the towers were 45 and 90 m a.g.l. at Ridge Hill, 54, 100 and 185 m a.g.l. at Tacolneston and 222 m a.g.l. at Angus. For stations with multiple inlets, each height was sampled sequentially. In this study, an average measurement of the two lowest heights was used (measurements from 185 m a.g.l. at Tacolneston were not used). Nitrous oxide observations at the telecommunication tower sites were made approximately every 10 min on a GC-ECD system, based on the system described in Ganesan et al. (2013) and Hall et al. (2011) and were calibrated on the SIO-98 scale. For the N₂O configuration, measurements at Ridge Hill and Tacolneston were only made at 90 and 100 m a.g.l., respectively.

Measurements were averaged over each two hour period and filtered for local influence using a transport model. Measurements corresponding to times when there was a high sensitivity of mole fractions to emissions from the nine grid cells surrounding the station (defined when total sensitivity exceeded a selected threshold) were removed from analysis, as they could lead to artifacts in the inversion. For CH₄ observations, measurement uncertainty described the variability of one-minute data in the two-hour averaging period. For N₂O observations, this uncertainty was the quadratic sum of the instrument precision (calculated as the SD of the approximately hourly measurements of the standard each day) and the variability in the averaging period. Typical instrumental uncertainties were 10 ppb CH₄ and 0.3 ppb N₂O. Model errors were estimated as part of the inversion framework.

3 Atmospheric transport model

The UK Met Office model, NAME III (Numerical Atmospheric dispersion Modelling Environment version 3, henceforth called NAME) was used to quantify the relationship between surface emissions and simulated measurements at each observation point and time. For each two hour period, NAME tracked particles backwards in time for 30 days and as particles were transported through the three-dimensional model, recorded the mass of particles and amount of time spent interacting with the first hundred meters a.g.l. (i.e., the surface). This directly provided the sensitivity of concentrations at the measurement site to surface emissions. Twenty thousand particles were released each hour at a source strength of 1 gs^{-1} . The model was driven by the Met Office's Unified Model (UM) analysis meteorology at $0.352^\circ \times 0.234^\circ$ resolution ($\sim 25 \text{ km}$) with 70 vertical levels. After July 2014, the resolution of the UM meteorology was increased to $\sim 17 \text{ km}$ but NAME output retained the original $\sim 25 \text{ km}$ resolution. The inversion domain extended from approximately 36 to 67° N and -14 to 31° E , covering the UK and most of continental Europe. For the purposes of estimating boundary conditions (discussed further in Sect. 4) a second, larger domain (9 to 81° N and -100 to 46° E) was used to identify the origins of air masses that entered the smaller inversion domain.

A complete description of NAME can be found in Ryall and Maryon (1998), Morrison and Webster (2005) and Jones et al. (2007) and of its use in trace gas emissions estimation in Manning et al. (2011).

4 Inversion framework

We followed the hierarchical Bayesian inversion methodology outlined in Ganesan et al. (2014) and extended this method to solve for additional hyper-parameters. This method allows for the systematic estimation of fluxes and critical uncertainty parameters, which was shown to result in a more complete characterization of uncertainties in the system.

ACPD

15, 857–886, 2015

Estimating UK greenhouse gas emissions

A. L. Ganesan et al.

Title Page

Abstract

Introduction

Conclusions

References

Tables

Figures



Back

Close

Full Screen / Esc

Printer-friendly Version

Interactive Discussion



scribed by Eq. (2), with s_{ij} representing the elements in spatial covariance matrix, \mathbf{S} . Γ is the gamma function and K_ν is the modified Bessel function of the second kind. When $\nu = 0.5$, the Matérn function becomes an exponential covariance function and when $\nu \gg 0.5$, it approaches a squared exponential function (similar to Gaussian).

$$t_{ij} = \sqrt{t_{ii}} \cdot \sqrt{t_{jj}} \cdot \exp\left(\frac{-t}{\tau}\right) \quad (1)$$

$$s_{ij} = \sqrt{s_{ii}} \cdot \sqrt{s_{jj}} \cdot \frac{1}{\Gamma(\nu)2^{\nu-1}} \left(\sqrt{2\nu\frac{d}{l}}\right)^\nu K_\nu\left(\sqrt{2\nu\frac{d}{l}}\right) \quad (2)$$

These hyper-parameters account for “uncertainties in uncertainties” and reduce the effect of subjective assumptions on a priori emissions uncertainties, model uncertainties and correlation scales. Fluxes, boundary conditions and hyper-parameters were informed by the data, z , through a Markov chain Monte Carlo (MCMC) framework, which has previously been shown to result in a more complete uncertainty quantification because these parameters and their uncertainties are passed systematically through the inversion (Ganesan et al., 2014; Rigby et al., 2011).

4.2 Boundary conditions

Boundary conditions were estimated for each of ten boundaries to the domain and represented the part of the measured concentration not simulated by the 30 day air histories. Multiple boundary conditions were estimated to represent the variable levels and directions that air enters the domain (for example, due to a north–south gradient). A schematic for these boundaries is provided in the Supplement.

The boundary condition to the west-south-west (WSW) edge was formulated as a polynomial shown by Eq. (3), with six sinusoidal terms, a linear trend term and an offset term.

$$\text{BC}_{\text{WSW}} = \sum_i^3 \left[a_i \cdot \sin\left(\frac{2\pi i(t - t_0)}{T}\right) + b_i \cdot \cos\left(\frac{2\pi i(t - t_0)}{T}\right) \right] + cx + d \quad (3)$$

however, that some of these measurements would be missing due to instrumental or site problems and \mathbf{y} is an additional parameter that is sampled in the MCMC chain and compared to observations through matrix \mathbf{C} . Therefore, we assume that errors in the model will be correlated even at times/locations that observations do not exist.

The joint distribution of \mathbf{x} , $\boldsymbol{\mu}_x$, $\boldsymbol{\sigma}_x$, $\boldsymbol{\sigma}_{yt}$, $\boldsymbol{\sigma}_{ys}$, τ , ν , l and \mathbf{y} is expressed through Eq. (8), through the hierarchical propagation of Bayes' theorem and the probability chain rule, where $\rho(\cdot)$ describes the prior PDF and $\rho(\cdot|\cdot)$ is a conditional of the first parameter given the second.

$$\rho(\mathbf{x}, \boldsymbol{\mu}_x, \boldsymbol{\sigma}_x, \boldsymbol{\sigma}_{yt}, \boldsymbol{\sigma}_{ys}, \tau, \nu, l, \mathbf{y} | \mathbf{z}, \mathbf{D}) \propto \rho(\mathbf{z} | \mathbf{y}, \mathbf{D}) \cdot \rho(\mathbf{y} | \mathbf{x}, \boldsymbol{\sigma}_{yt}, \boldsymbol{\sigma}_{ys}, \tau, \nu, l) \cdot \rho(\mathbf{x} | \boldsymbol{\mu}_x, \boldsymbol{\sigma}_x) \cdot \rho(\boldsymbol{\mu}_x) \cdot \rho(\boldsymbol{\sigma}_x) \cdot \rho(\boldsymbol{\sigma}_{yt}) \cdot \rho(\boldsymbol{\sigma}_{ys}) \cdot \rho(\tau) \cdot \rho(\nu) \cdot \rho(l) \quad (8)$$

As shown in Eq. (8), each hyper-parameter ($\boldsymbol{\mu}_x$, $\boldsymbol{\sigma}_x$, $\boldsymbol{\sigma}_{yt}$, $\boldsymbol{\sigma}_{ys}$, τ , ν , l) requires an "a priori" PDF to be specified. Through MCMC, these PDFs are sampled from and used to form the posterior PDF. The lognormal distribution (LN) was used for \mathbf{x} , $\boldsymbol{\mu}_x$, $\boldsymbol{\sigma}_x$, $\boldsymbol{\sigma}_y$ and $\boldsymbol{\sigma}_{ys}$ to represent skewed distributions that are not defined for negative values. This prevents unphysical solutions from being reached. A uniform distribution (U) was used as a non-informative prior for correlation hyper-parameters, τ , ν and l . Model and measurement uncertainties were assumed to be Gaussian (N) as it was assumed that these random errors were symmetric around the median. Regions that contained a net sink (for N_2O , some oceanic areas are sinks at certain times of the year) were estimated with Gaussian distributions.

By assimilating data from multiple sites and at high-frequency, the size of the estimation problem can get very large for MCMC. To reduce the computational cost of multiplying, inverting and computing the determinant of large matrices over 50 000 iterations, it was assumed that the covariance matrix, \mathbf{R} , was separable in space and time (Eq. 9). This has been widely employed in geostatistics, where it is assumed that correlations in time are not dependent on position and correlations in space are not dependent on time (e.g., Meirink et al., 2008; Thompson et al., 2011; Yadav and Michalak,

Estimating UK greenhouse gas emissions

A. L. Ganesan et al.

Title Page

Abstract

Introduction

Conclusions

References

Tables

Figures



Back

Close

Full Screen / Esc

Printer-friendly Version

Interactive Discussion



2013).

$$\mathbf{R}(t, t + \Delta_t, s, s + \Delta_s) = \mathbf{T}(t, t + \Delta_t)\mathbf{S}(s, s + \Delta_s) \quad (9)$$

By assuming separability in the covariance matrix, we could exploit the following properties:

1. $\mathbf{R} = \mathbf{T} \otimes \mathbf{S}$, where separable square matrix \mathbf{R} of size mn can be written as the Kronecker product of two matrices governing the temporal and spatial covariances, respectively. \mathbf{T} is a square matrix of size m and \mathbf{S} is a square matrix of size n .
2. $\mathbf{R}^{-1} = (\mathbf{T} \otimes \mathbf{S})^{-1} = \mathbf{T}^{-1} \otimes \mathbf{S}^{-1}$, so the computation of the inverse of a square matrix of size mn can be decomposed into the inverse of two smaller matrices.
3. $\det(\mathbf{R}) = \det(\mathbf{T} \otimes \mathbf{S}) = \det(\mathbf{T})^n \det(\mathbf{S})^m$, so the computation of the determinant of a square matrix of size mn can be decomposed into the determinant of two smaller similar matrices.
4. $\mathbf{a} = \mathbf{R}^{-1}\mathbf{b}$, where \mathbf{a} and \mathbf{b} are vectors of length mn . In this analysis, \mathbf{b} represents residual vectors $(\mathbf{y} - \mathbf{H}\mathbf{x})$ and $(\mathbf{z} - \mathbf{C}\mathbf{y})$ and \mathbf{a} represents the vector required to compute the likelihoods in Eq. (8). This operation can now be computed as $\mathbf{A} = \mathbf{S}^{-1} \mathbf{B} \mathbf{T}^{-1T}$, where \mathbf{B} is an array composed of \mathbf{b} reordered to size $n \times m$ and \mathbf{A} , also of dimension $n \times m$ can be restacked to form \mathbf{a} . The advantage of this computation is that the Kronecker product forming \mathbf{R} does not need to be explicitly computed and the product of the (large) covariance matrix and vector can be reformulated as the product of smaller arrays.

Because the computational cost of these operations are approximately of the order n^3 , assuming separability makes a dramatic improvement in efficiency for MCMC.

4.4 A priori values

Tables 1 and 2 describe the a priori median values for all of the hyper-parameters of the system (with the superscript μ referring to the median of that respective distribution). Hyper-parameter SDs of the lognormal distributions (denoted by superscript σ), μ_x^σ , σ_x^σ , σ_{yt}^σ and σ_{ys}^σ were calculated to be the value that resulted in half to 1.5 times the median being contained between the 5th and 95th percentiles. Gridded anthropogenic emissions for the UK were from the NAEI for 2012. Anthropogenic emissions for other countries were taken from the Emission Database for Global Atmospheric Research version 4.2 (EDGAR, JRC/PBL, 2011) but these emissions were scaled by country to the UNFCCC reported total emissions to maintain consistency with the numbers reported by individual countries.

5 Results

We present top-down CH_4 and N_2O emissions for the UK and Ireland from August 2012 to August 2014 along with an analysis of the uncertainty parameters derived in the inversion. Uncertainties provided for all parameters correspond to the 5th to 95th percentile range. In addition, the simulated posterior time series, derived baselines and comparison with observations are provided in the Supplement.

Figure 2 shows CH_4 and N_2O emissions by month over the study period. On average, the UK's emissions were 2.08 (1.72 – 2.47) Tgyr^{-1} CH_4 and 0.105 (0.087 – 0.127) Tgyr^{-1} N_2O and Ireland's emissions were 0.62 (0.52 – 0.73) Tgyr^{-1} CH_4 and 0.027 (0.024 – 0.031) Tgyr^{-1} N_2O . Both UK CH_4 and N_2O emissions were almost continuously lower than the prior. Methane emissions between February and May 2013 were the most uncertain due to missing data from Angus and similarly, N_2O emissions in December 2012 and January 2013 had larger uncertainties than other times of the year due to the fact that the N_2O instrumentation at Ridge Hill was down during those

Title Page

Abstract

Introduction

Conclusions

References

Tables

Figures



Back

Close

Full Screen / Esc

Printer-friendly Version

Interactive Discussion



two months. Larger uncertainties at times when stations are not available highlights the increased observational constraint provided by the full network.

While CH_4 emissions do not show significant seasonality, N_2O in contrast has a pronounced seasonal cycle, with a maximum in the summer months and minimum in the winter. Though the a priori emissions have a small seasonal cycle due to the natural soil and oceanic sources of N_2O , the derived amplitude of approximately 0.05 Tg yr^{-1} is much larger in the posterior estimates and we will discuss this seasonality further.

Figures 3 and 4 show spatial maps of median derived emissions for the two gases over the study period, the percentage difference from the prior and the fractional uncertainties (ratio of the difference between 5th and 95th percentiles to the median) derived in the inversion. Dots in the difference map indicates regions where the difference was statistically significant (i.e., the prior was outside the 5th to 95th percentile range of the posterior emissions). Spatial maps of the prior emissions field for the UK NAEI for the dominant emissions sectors are shown in Fig. 1. Comparison of the posterior emissions distribution with the sectoral inventory maps allows us to determine whether differences between the top-down and bottom-up emissions can be attributed to particular sectors.

The two dominant and approximately equivalent sources of CH_4 in the UK are agriculture (cattle, manure) and waste (landfill) sectors, each contributing about 44 and 40% respectively to the national emissions total from the NAEI inventory. While agricultural sources are more diffuse than landfill sources, the maps for the waste sector show a distinct spatial pattern. The waste sector dominates emissions from the eastern and central England. Agricultural emissions are generally well-distributed around the country with the highest emissions in western England, Wales, Northern Ireland and southern Scotland, in grassland regions where livestock production is prevalent. While emissions from the entire domain are generally lower than the prior, the largest difference, as a percentage of the prior, occurs throughout Scotland, western England and eastern Ireland. An analysis of the uncertainties derived for each region for each month shows these differences to be statistically significant, with the prior lying outside the 5th

Estimating UK greenhouse gas emissions

A. L. Ganesan et al.

Title Page

Abstract

Introduction

Conclusions

References

Tables

Figures



Back

Close

Full Screen / Esc

Printer-friendly Version

Interactive Discussion



to 95th percentile range of the posterior distribution. These results suggests that the agricultural sector due to its prevalence in those regions, may be overestimated in the inventory.

The prior for N_2O , which is overwhelmingly from agriculture, is also generally higher than our estimated emissions. In our seasonal analysis (Fig. 5), we find the largest differences in winter (DJF), which in part is because there is no seasonal cycle represented in the anthropogenic component of the prior. In the winter, the difference from the prior is statistically significant throughout most of the land regions of the UK and Ireland. The NAEI sectoral distribution for agricultural N_2O shows that emissions are relatively evenly spread around the country, with emissions generally being from fertilized grasslands in the west of England and from fertilized arable land, pig and poultry production in the East. While emissions throughout the UK and Ireland grow toward spring and summer, spatial maps of the posterior emissions show the largest emissions in eastern England during the spring and in central England during the summer. A study over one UK sheep-grazed grassland, which was fertilized three times over the spring and summer, showed fertilizer N_2O emissions to last from one to three weeks, following fertilizer application, with the maximum emission occurring in July (Skiba et al., 2012). However, emissions depend strongly not only on fertilizer application, but also on precipitation and temperature and these can have strong regional differences as well as year-to-year variability. These findings suggest that the pronounced seasonal cycle is likely to due seasonality in fertilized soils as well as seasonality in environmental drivers, which are not reflected in the annual resolution NAEI inventory.

Analysis of the uncertainties derived in the inversion (panel c of Figs. 3 and 4) shows the greatest observational constraint in the ~ 100 km around the stations, which predominantly constrain southern and central England and western Ireland. Uncertainties for N_2O emissions are typically larger than for CH_4 emissions, likely due to the lower signal-to-noise of N_2O observations (i.e., CH_4 is measured with higher precision and pollution events are larger). For CH_4 , an increase in emissions was found to occur in Wales. While the difference from the prior was not statistically significant (i.e., the frac-

Estimating UK greenhouse gas emissions

A. L. Ganesan et al.

[Title Page](#)[Abstract](#)[Introduction](#)[Conclusions](#)[References](#)[Tables](#)[Figures](#)[Back](#)[Close](#)[Full Screen / Esc](#)[Printer-friendly Version](#)[Interactive Discussion](#)

tional difference from the prior each month typically lay within the 5 to 95 percentiles), the posterior uncertainty showed that the region is well-constrained by the network (and primarily by Ridge Hill). For this region covering eastern Wales, there was considerable month-to-month variability (about half of the months during the period showed this increase and half did not). This is likely caused by poorly resolved meteorology around two large point sources (Cardiff and Swansea) that are surrounded by mountains just to the west of Ridge Hill. This feature could be improved with a more highly resolved grid and/or meteorology in that region.

Figure 6 shows derived uncertainties for each site. These uncertainties could be due to model error or any unresolved processes in the inversion. The median posterior value is shown, with error bars indicating the 5th and 95th percentile solutions. On average, uncertainties for the CH₄ and N₂O studies were ~ 20 ppb and 0.4 ppb, respectively. For the CH₄ study, Tacolneston consistently exhibited the largest error, the cause of which could be from two factors: the largest CH₄ pollution events are measured at Tacolneston and there are known nearby sources (gas fields in the North Sea and landfills in east England) with sporadic emissions that may not be reflected in the temporally constant NAEI prior or resolved in the monthly inversion. Mace Head and Angus have the smallest uncertainties, both due to the smaller magnitude of pollution at these sites and due to the more constant regional emissions sources. The increased uncertainty at Tacolneston is reflected in the emissions uncertainties shown in panel c of Fig. 3; uncertainties in the regions surrounding Tacolneston are greater than in the regions surrounding other stations. This feature also highlights that the uncertainties in the various components of the inversion are passed systematically through the inversion to emissions and emission uncertainties. Uncertainties derived for N₂O are similar for both Tacolneston and Ridge Hill, likely due to both sites generally measuring agricultural emissions, and further suggests that the increased CH₄ error at Tacolneston is due to unresolved emissions processes rather than model error at that site. NAME has previously been validated against tracer release experiments, surface and balloon measurements but parametric and structural uncertainties are not well known

Estimating UK greenhouse gas emissions

A. L. Ganesan et al.

[Title Page](#)[Abstract](#)[Introduction](#)[Conclusions](#)[References](#)[Tables](#)[Figures](#)[Back](#)[Close](#)[Full Screen / Esc](#)[Printer-friendly Version](#)[Interactive Discussion](#)

(Morrison and Webster, 2005; Ryall and Maryon, 1998). While the results of this study cannot discern specific sources of error in the model, this is a subject of great interest and future work.

Spatial and temporal correlation scales were also derived for the two gases. The correlation scales are related to a number of factors: errors in the model transport (e.g., a misplaced weather front at one time will likely be misplaced a short time later) as well as unresolved emissions processes (e.g., errors in the assumption of constant emissions). The two sources of correlated errors cannot be disentangled but the time and length scales derived in the inversion are a measure of the scales of the missing or erroneous processes. Average correlation scales of 1.0 (0.72–1.43) days and 133 (15–317) km were derived over the period for the CH₄ study and 2.6 (1.9–3.9) days and 228 (25–450) km for the N₂O study. The scales are more tightly constrained for CH₄ than for N₂O, likely due to the higher signal-to-noise of the observations. The spatial correlation scale is not well-constrained for N₂O and reflects the prior distribution, indicating that there is not enough information in the network to constrain this parameter. The correlation timescale is smaller for CH₄ than for N₂O. Though there are differences in the two networks (i.e., N₂O is not measured at Angus), a CH₄ inversion in which Angus was excluded was also performed and similar correlation scales were derived (Supplement), suggesting that the network differences are not the source of differences in correlation scales. Furthermore, because the same transport model was used for the two studies, model errors were expected to be similar for the two gases so the differences are likely due to unresolved emissions in the prior. We noted the increased variances at Tacolneston and speculated that this was due to sporadic emissions from landfills and offshore gas that were not modeled by the constant prior emissions field and not resolved in the inversion. The longer timescale for N₂O suggests that unresolved emission characteristics from fertilizers acts on a slightly longer timescale (several days). The correlation length scale of 133 km for CH₄ suggests that the current network, with the nearest two stations being ~ 250 km apart, could benefit from additional stations to further constrain CH₄ emissions. Given the typical correlation scales that were derived

Estimating UK greenhouse gas emissions

A. L. Ganesan et al.

Title Page

Abstract

Introduction

Conclusions

References

Tables

Figures



Back

Close

Full Screen / Esc

Printer-friendly Version

Interactive Discussion



Estimating UK greenhouse gas emissions

A. L. Ganesan et al.

Title Page

Abstract

Introduction

Conclusions

References

Tables

Figures



Back

Close

Full Screen / Esc

Printer-friendly Version

Interactive Discussion



verification of emissions at the country-level, methods need to be employed that account for these important parameters. Through this hierarchical inversion framework, we inferred model errors and uncertainty correlation scales and propagated these uncertainties into the emissions estimates. Model errors for the two studies were on average approximately 20 and 0.4 ppb, respectively, but showed variations from site to site and for different times depending on the meteorology. We derived the largest CH₄ model errors at Tacolneston, likely due to its proximity to gas extraction in the North Sea and landfills in east England, sources which have sporadic emissions characteristics that are not simulated. We inferred temporal and spatial correlation scales of 1.0 (0.72–1.43) days and 133 (15–317) km for the CH₄ network and 2.6 (1.9–3.9) days and 228 (25–450) km for the N₂O network, with differences in the two studies likely being due to differences in unresolved emissions processes.

The Supplement related to this article is available online at doi:10.5194/acpd-15-857-2015-supplement.

Acknowledgements. This modeling study was funded by the UK Department of Energy and Climate Change (DECC) grant GA0201 to the University of Bristol. Operations at Mace Head, Ridge Hill, Tacolneston and Angus were funded by DECC grant GA0201 and partly by the InGOS EU project (284274). Additionally, measurements at Mace Head were also partially funded from NASA grant NNX11AF17G to the Massachusetts Institute of Technology, which supports the Advanced Global Atmospheric Gases Experiment (AGAGE) and at Tacolneston through the NERC National Centre for Atmospheric Research. Calibration of Mace Head data was made possible by NASA grant NNX11AF15G to the Scripps Institution of Technology. The UK National Atmospheric Emissions Inventory (NAEI) was funded by DECC, the Department for Environment, Food and Rural Affairs (Defra), the Scottish Government, the Welsh Government and the Northern Ireland Department of Environment. We are grateful to the station technicians, Gerard Spain (Mace Head), Stephen Humphrey (Tacolneston), Emanuel Blei (Angus, 2013–present) and Rab Howard (Angus, 2012–2013) for maintaining site and instrumental operations and to Matt Rigby for productive discussions on the inverse modeling.

References

- Bergamaschi, P., Corazza, M., Karstens, U., Athanassiadou, M., Thompson, R. L., Pison, I., Manning, A. J., Bousquet, P., Segers, A., Vermeulen, A. T., Janssens-Maenhout, G., Schmidt, M., Ramonet, M., Meinhardt, F., Aalto, T., Haszpra, L., Moncrieff, J., Popa, M. E., Lowry, D., Steinbacher, M., Jordan, A., O'Doherty, S., Piacentino, S., and Dlugokencky, E.: Top-down estimates of European CH₄ and N₂O emissions based on four different inverse models, *Atmos. Chem. Phys. Discuss.*, 14, 15683–15734, doi:10.5194/acpd-14-15683-2014, 2014. 860
- Bloom, A. A., Palmer, P. I., Fraser, A., and Reay, D. S.: Seasonal variability of tropical wetland CH₄ emissions: the role of the methanogen-available carbon pool, *Biogeosciences*, 9, 2821–2830, doi:10.5194/bg-9-2821-2012, 2012. 879
- Bousquet, P., Ciais, P., Miller, J., Dlugokencky, E., Hauglustaine, D., Prigent, C., Van der Werf, G., Peylin, P., Brunke, E., Carouge, C., Langenfelds, R. L., Lathière, J., Papa, F., Ramonet, M., Schmidt, M., Steele, L. P., Tyler, S., and White, J.: Contribution of anthropogenic and natural sources to atmospheric methane variability, *Nature*, 443, 439–443, 2006. 879
- Corazza, M., Bergamaschi, P., Vermeulen, A. T., Aalto, T., Haszpra, L., Meinhardt, F., O'Doherty, S., Thompson, R., Moncrieff, J., Popa, E., Steinbacher, M., Jordan, A., Dlugokencky, E., Brühl, C., Krol, M., and Dentener, F.: Inverse modelling of European N₂O emissions: assimilating observations from different networks, *Atmos. Chem. Phys.*, 11, 2381–2398, doi:10.5194/acp-11-2381-2011, 2011. 860
- Fung, I., John, J., Lerner, J., Matthews, E., Prather, M., Steele, L. P., and Fraser, P. J.: Three-dimensional model synthesis of the global methane cycle, *J. Geophys. Res.*, 96, 13033–13065, doi:10.1029/91JD01247, 1991. 879
- Ganesan, A. L., Chatterjee, A., Prinn, R. G., Harth, C. M., Salameh, P. K., Manning, A. J., Hall, B. D., Mühle, J., Meredith, L. K., Weiss, R. F., O'Doherty, S., and Young, D.: The variability of methane, nitrous oxide and sulfur hexafluoride in Northeast India, *Atmos. Chem. Phys.*, 13, 10633–10644, doi:10.5194/acp-13-10633-2013, 2013. 862
- Ganesan, A. L., Rigby, M., Zammit-Mangion, A., Manning, A. J., Prinn, R. G., Fraser, P. J., Harth, C. M., Kim, K.-R., Krummel, P. B., Li, S., Mühle, J., O'Doherty, S. J., Park, S., Salameh, P. K., Steele, L. P., and Weiss, R. F.: Characterization of uncertainties in atmospheric trace gas inversions using hierarchical Bayesian methods, *Atmos. Chem. Phys.*, 14, 3855–3864, doi:10.5194/acp-14-3855-2014, 2014. 861, 863, 865

ACPD

15, 857–886, 2015

Estimating UK greenhouse gas emissions

A. L. Ganesan et al.

Title Page

Abstract

Introduction

Conclusions

References

Tables

Figures



Back

Close

Full Screen / Esc

Printer-friendly Version

Interactive Discussion



Estimating UK greenhouse gas emissions

A. L. Ganesan et al.

Title Page

Abstract

Introduction

Conclusions

References

Tables

Figures



Back

Close

Full Screen / Esc

Printer-friendly Version

Interactive Discussion



Hall, B. D., Dutton, G. S., Mondeel, D. J., Nance, J. D., Rigby, M., Butler, J. H., Moore, F. L., Hurst, D. F., and Elkins, J. W.: Improving measurements of SF₆ for the study of atmospheric transport and emissions, *Atmos. Meas. Tech.*, 4, 2441–2451, doi:10.5194/amt-4-2441-2011, 2011. 862

5 Jones, A., Thomson, D. J., Hort, M. C., and Devenish, B.: The UK Met Office's next-generation atmospheric dispersion model, NAME III, in: *Air Pollution Modeling and Its Application XVII*, edited by: Borrego, C. and Norman, A.-L., Springer, New York, USA., 580–589, 2007. 863

JRC/PBL: Joint Research Centre of the European Commission (JRC) /Netherlands Environmental Assessment Agency (PBL), Emission Database for Global Atmospheric Research (EDGAR), release version 4.2, available at: <http://edgar.jrc.ec.europa.eu> (12 May 2014) 2011. 869, 879, 880

Manizza, M., Keeling, R. F., and Nevison, C. D.: On the processes controlling the seasonal cycles of the air-sea fluxes of O₂ and N₂O: a modelling study, *Tellus B*, 64, 18429, doi:10.3402/tellusb.v64i0.18429, 2012. 880

15 Manning, A. J., O'Doherty, S., Jones, A. R., Simmonds, P. G., and Derwent, R. G.: Estimating UK methane and nitrous oxide emissions from 1990 to 2007 using an inversion modeling approach, *J. Geophys. Res.*, 116, D02305, doi:10.1029/2010JD014763, 2011. 860, 863

Meirink, J. F., Bergamaschi, P., and Krol, M. C.: Four-dimensional variational data assimilation for inverse modelling of atmospheric methane emissions: method and comparison with synthesis inversion, *Atmos. Chem. Phys.*, 8, 6341–6353, doi:10.5194/acp-8-6341-2008, 2008. 20 867

Morrison, N. L. and Webster, H. N.: An assessment of turbulence profiles in rural and urban environments using local measurements and numerical weather prediction results, *Bound.-Lay. Meteorol.*, 115, 223–239, doi:10.1007/s10546-004-4422-8, 2005. 863, 873

25 Myhre, G., Shindell, D., Bréon, F.-M., Collins, W., Fuglestvedt, J., Huang, J., Koch, D., Lamarque, J.-F., Lee, D., Mendoza, B., Nakajima, T., Robock, A., Stephens, G., Takemura, T., and Zhang, H.: Anthropogenic and natural radiative forcing, in: *Climate Change 2013: The Physical Science Basis. Contribution of Working Group I to the Fifth Assessment Report of the Intergovernmental Panel on Climate Change*, edited by: Stocker, T. F., Qin, D., Plattner, G.-K., Tignor, M., Allen, S. K., Boschung, J., Nauels, A., Xia, Y., Bex, V., and Midgley, P. M., Cambridge University Press, Cambridge, United Kingdom and New York, NY, USA, 659–740, 2013. 859

**Estimating UK
greenhouse gas
emissions**

A. L. Ganesan et al.

Title Page

Abstract

Introduction

Conclusions

References

Tables

Figures



Back

Close

Full Screen / Esc

Printer-friendly Version

Interactive Discussion



Prather, M. J., Holmes, C. D., and Hsu, J.: Reactive greenhouse gas scenarios: systematic exploration of uncertainties and the role of atmospheric chemistry, *Geophys. Res. Lett.*, 39, L09803, doi:10.1029/2012GL051440, 2012. 860

Prinn, R. G., Weiss, R. F., Fraser, P. J., Simmonds, P. G., Cunnold, D. M., Alyea, F. N., O'Doherty, S., Salameh, P., Miller, B. R., Huang, J., Wang, R. H. J., Hartley, D. E., Harth, C., Steele, L. P., Sturrock, G., Midgley, P. M., and McCulloch, A.: A history of chemically and radiatively important gases in air deduced from ALE/GAGE/AGAGE, *J. Geophys. Res.*, 105, 17751–17792, doi:10.1029/2000JD900141, 2000. 861

Rigby, M., Manning, A. J., and Prinn, R. G.: Inversion of long-lived trace gas emissions using combined Eulerian and Lagrangian chemical transport models, *Atmos. Chem. Phys.*, 11, 9887–9898, doi:10.5194/acp-11-9887-2011, 2011. 865

Ryall, D. B. and Maryon, R. H.: Validation of the UK Met. Office's name model against the ETEX dataset, *Atmos. Environ.*, 32, 4265–4276, doi:10.1016/S1352-2310(98)00177-0, 1998. 863, 873

Saikawa, E., Schlosser, C. A., and Prinn, R. G.: Global modeling of soil nitrous oxide emissions from natural processes, *Global Biogeochem. Cy.*, 27, 972–989, doi:10.1002/gbc.20087, 2013. 880

Skiba, U., Jones, S. K., Dragosits, U., Drewer, J., Fowler, D., Rees, R. M., Pappa, V. A., Cardenas, L., Chadwick, D., Yamulki, S., and Manning, A. J.: UK emissions of the greenhouse gas nitrous oxide., *Philos. T. Roy. Soc. B*, 367, 1175–1185, doi:10.1098/rstb.2011.0356, 2012. 871

Thompson, R. L., Gerbig, C., and Rödenbeck, C.: A Bayesian inversion estimate of N₂O emissions for western and central Europe and the assessment of aggregation errors, *Atmos. Chem. Phys.*, 11, 3443–3458, doi:10.5194/acp-11-3443-2011, 2011. 867

van der Werf, G. R., Randerson, J. T., Giglio, L., Collatz, G. J., Mu, M., Kasibhatla, P. S., Morton, D. C., DeFries, R. S., Jin, Y., and van Leeuwen, T. T.: Global fire emissions and the contribution of deforestation, savanna, forest, agricultural, and peat fires (1997–2009), *Atmos. Chem. Phys.*, 10, 11707–11735, doi:10.5194/acp-10-11707-2010, 2010. 879, 880

Yadav, V. and Michalak, A. M.: Improving computational efficiency in large linear inverse problems: an example from carbon dioxide flux estimation, *Geosci. Model Dev.*, 6, 583–590, doi:10.5194/gmd-6-583-2013, 2013. 867

Estimating UK greenhouse gas emissions

A. L. Ganesan et al.

Title Page

Abstract Introduction

Conclusions References

Tables Figures

⏪ ⏩

◀ ▶

Back Close

Full Screen / Esc

Printer-friendly Version

Interactive Discussion

Table 1. A priori values of hyper-parameters used in the CH₄ study. Superscript μ denotes that these are the median values of the distribution.

Parameter	Category	Prior
x^μ	Anthropogenic Biomass burning Wetlands and rice Other natural Soil sink	NAEI or 2008 EDGAR 4.2 scaled to UNFCCC (JRC/PBL, 2011); 2008 emissions from GFED v 3.1 (van der Werf et al., 2010); 2008 emissions from Bloom et al. (2012); Fung et al. (1991); Bousquet et al. (2006);
x^μ	Polynomial baseline Offsets	Fit to statistically observed baseline at Mace Head over 2012–2013; Median fraction-weighted difference between upper air influenced observations and baseline or zero for horizontal directions;
σ_x^μ	Emissions	Lognormal SD corresponding to national scale emissions uncertainty of 50 %;
σ_x^μ	Polynomial baseline Offsets	Uncertainties from fit calculation; 10 ppb;
σ_{yt}^μ σ_{ys}^μ		SD of observations at all sites in 2 day period; SD of observations at each site over the month;
τ^μ		2 days (typical duration of pollution events);
v^μ		0.5 (exponential);
μ		250 km (smallest distance between the four measurement sites)



Estimating UK greenhouse gas emissions

A. L. Ganesan et al.

Title Page

Abstract Introduction

Conclusions References

Tables Figures

⏪ ⏩

◀ ▶

Back Close

Full Screen / Esc

Printer-friendly Version

Interactive Discussion

Table 2. Same as Table 1 but for N₂O.

Parameter	Category	Prior
x^μ	Anthropogenic Biomass burning Natural soils Ocean	NAEI or 2008 EDGAR 4.2 scaled to UNFCCC (JRC/PBL, 2011); 2008 emissions from GFED v 3.1 (van der Werf et al., 2010); 2008 emissions from Saikawa et al. (2013); Manizza et al. (2012);
x^μ	Polynomial baseline Offsets	Fit to statistically observed baseline at Mace Head over 2012–2013; Median fraction-weighted difference between upper air influenced observations and baseline or zero for horizontal directions;
σ_x^μ	Emissions	Lognormal SD corresponding to national scale emissions uncertainty of 100 %;
σ_x^μ	Polynomial baseline Offsets	Uncertainties from fit calculation; 2 ppb;
σ_{yt}^μ σ_{ys}^μ		SD of observations at all sites in 2 day period; SD of observations at each site over the month;
τ		2 days (typical duration of pollution events);
ν		0.5 (exponential function);
l		250 km (smallest distance between the four measurement sites)



Estimating UK greenhouse gas emissions

A. L. Ganesan et al.

Title Page

Abstract

Introduction

Conclusions

References

Tables

Figures



Back

Close

Full Screen / Esc

Printer-friendly Version

Interactive Discussion

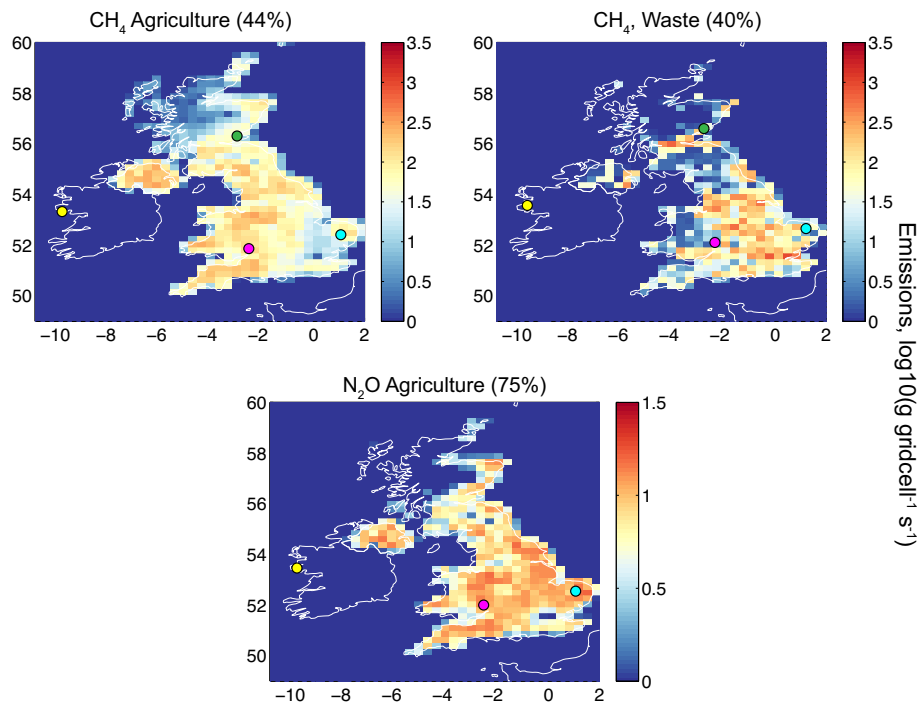


Figure 1. National Atmospheric Emissions Inventory maps for the major emission sources of CH_4 and N_2O . Colored circles show the measurement stations (MHD, yellow; RGL, magenta; TAC, cyan; TTA, green).

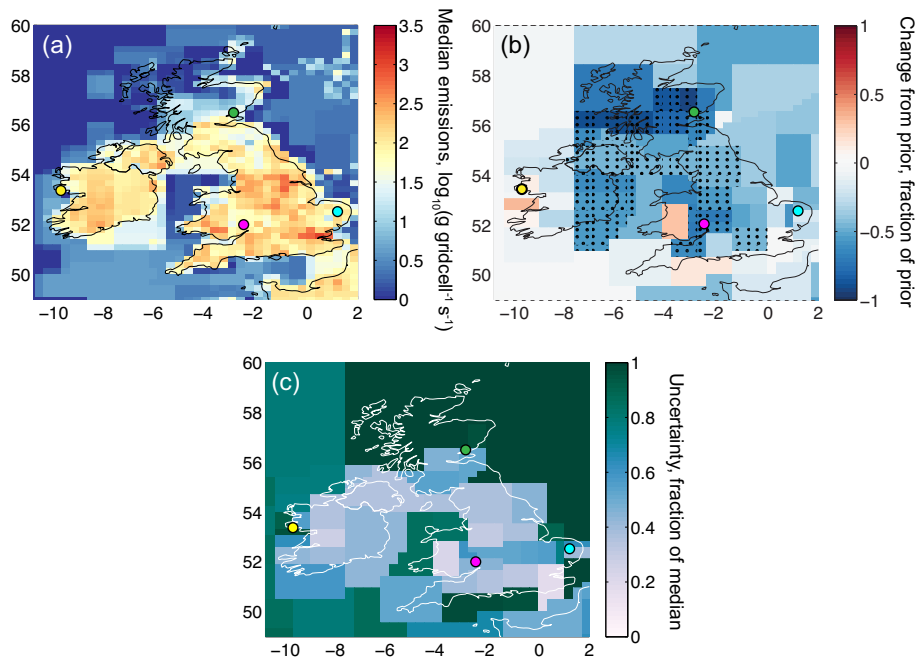


Figure 3. (a) Median posterior CH_4 emissions shown on a logarithmic scale. Emissions have been disaggregated from the larger regions estimated in the inversion using the prior distribution. (b) Fractional difference of the median posterior emissions from the prior (relative to the prior). Dots show statistically significant differences, where the prior emissions lie outside of the 5th to 95th percentile range of the posterior emissions. (c) Fractional posterior emissions uncertainty. This corresponds to the average difference between the median and the 5th and 95th percentiles, relative to the median. Colored circles show the measurement stations (MHD, yellow; RGL, magenta; TAC, cyan; TTA, green).

Estimating UK greenhouse gas emissions

A. L. Ganesan et al.

Title Page

Abstract

Introduction

Conclusions

References

Tables

Figures



Back

Close

Full Screen / Esc

Printer-friendly Version

Interactive Discussion



Estimating UK greenhouse gas emissions

A. L. Ganesan et al.

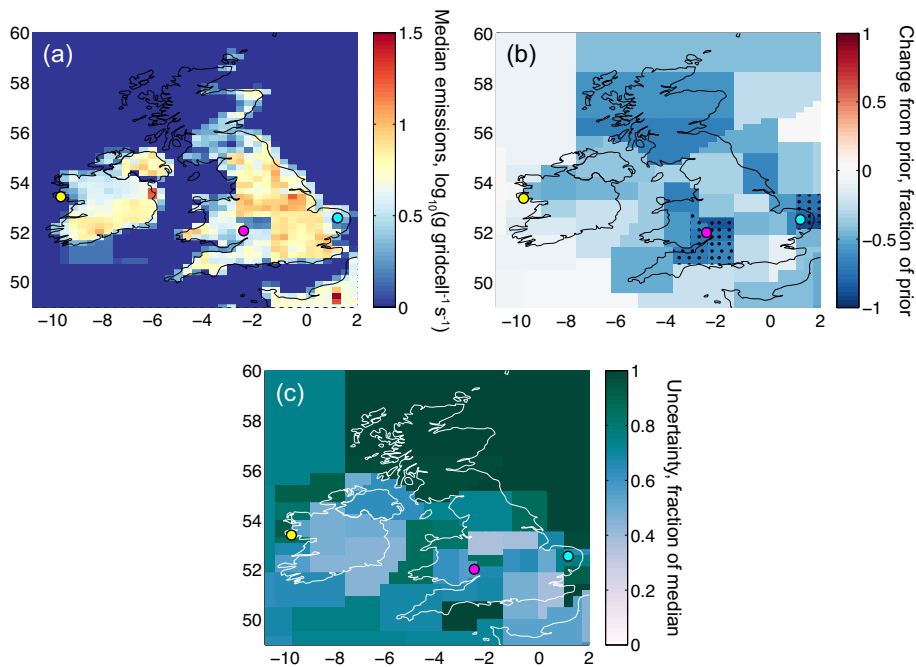


Figure 4. Same as Fig. 3 but for N₂O.

Title Page	
Abstract	Introduction
Conclusions	References
Tables	Figures
◀	▶
◀	▶
Back	Close
Full Screen / Esc	
Printer-friendly Version	
Interactive Discussion	



Estimating UK greenhouse gas emissions

A. L. Ganesan et al.

Title Page

Abstract

Introduction

Conclusions

References

Tables

Figures



Back

Close

Full Screen / Esc

Printer-friendly Version

Interactive Discussion

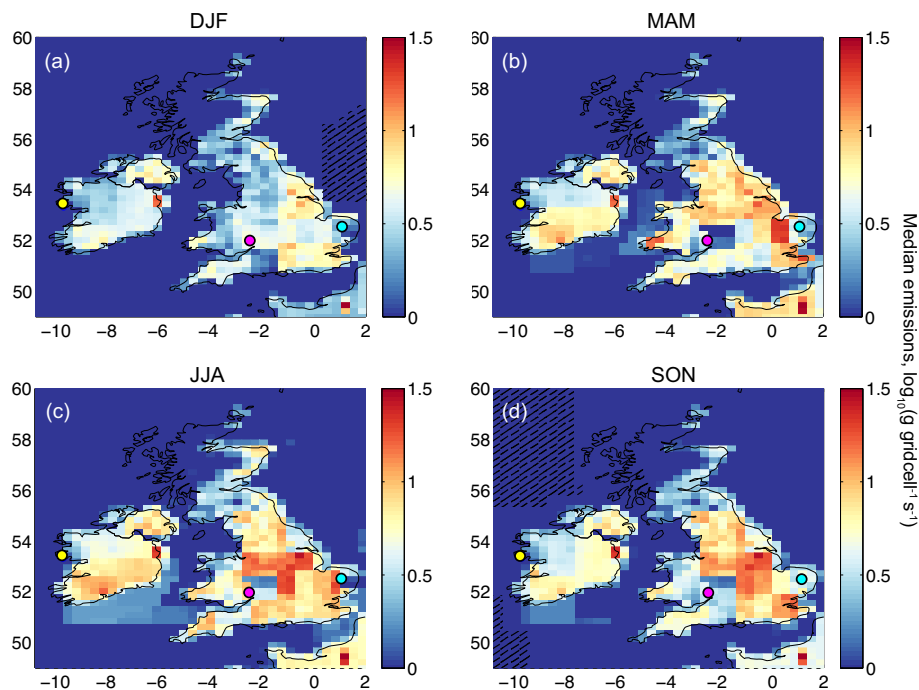


Figure 5. N₂O emissions by season, shown on a logarithmic scale. Emissions have been disaggregated from the larger regions estimated in the inversion using the prior distribution. Regions with hashing correspond to sink regions and are plotted as their absolute value. Colored circles show the measurement stations (MHD, yellow; RGL, magenta; TAC, cyan).

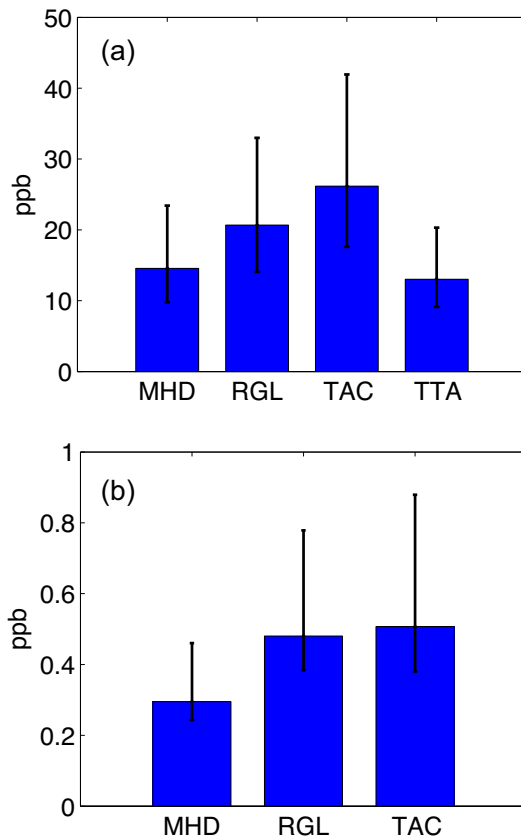


Figure 6. Median (a) CH₄ and (b) N₂O model uncertainties derived for each site. Error bars show the 5th to 95th percentile range.

Title Page

Abstract

Introduction

Conclusions

References

Tables

Figures



Back

Close

Full Screen / Esc

Printer-friendly Version

Interactive Discussion

